HETEK

Curing
Phase 2: Evaluation of Test Results

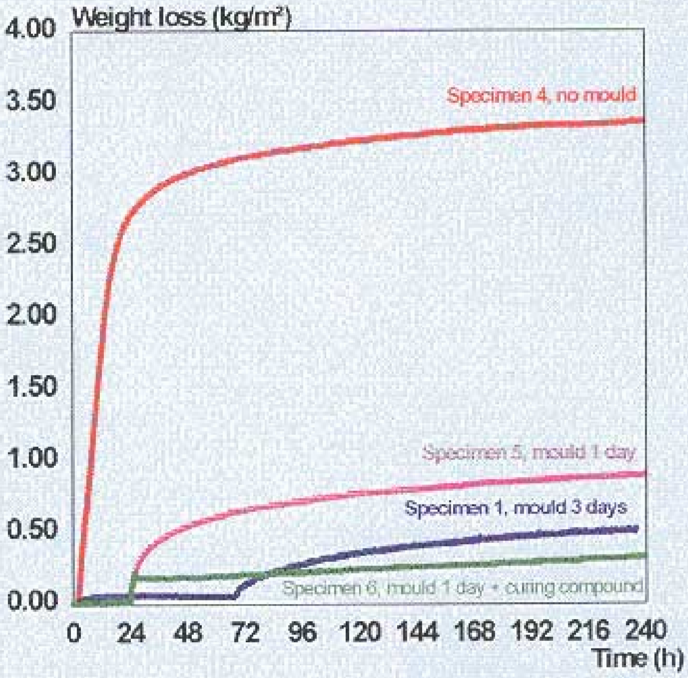

Report No.100
1997

Road Directorate Denmark Ministry of Transport

IRRD Information

Title in English	HETEK - Curing - Phase 2: Evaluation of Test Results
Title in Danish	HETEK - Efterbehandling - Fase 2: Evaluering af resultater
Authors	Tommy Nielsen and Marlene Haugaard
Subject classification	Field 32 Concrete

Key words

Key words	Concrete	4755
	Curing	3678
	Surface	6438
	Quality	9063
	Test methods	6288
	Evaluation	9020
	Denmark	8028

Abstract

This report forms a part of the Danish Road Directorate's research programme called High Performance Concrete - The Contractor's Technology (abbreviated to HETEK). HETEK is divided into eight parts where part No. 6 concerns Curing.

Part 6 is divided into a state of the art, a supplementary research, the phases 1 to 4, a main report and a guideline. Phase 2: Evaluation of Test Results, evaluates the results of the tests performed in phase 1.

The tests performed in phase 1 include measurement of water loss from 14 specimens during 10 days as a function of time while they were subjected to different curing methods. After 28 days samples were cut from the specimens and four types of tests were performed to investigate the effect of the different curing methods. These four tests were: Crack formation, chloride penetration, capillary water absorption and carbonation depth (accelerated test).

The basic hypothesis is that the results of these tests depend on a decreased hydration of the cement paste and hereby the structure formation, caused by the water loss.

The results of the evaluation were that only chloride penetration and partly carbonation depth could be correlated to the water loss and structure formation. The crack formation and the capillary water absorption showed weak correlation to the water loss.

UDK 624.012.4 621.795 693.548

ISSN 09 09 4288

ISBN 87 7491 8109

List of Contents

0. Preface **1**

1. Introduction **3**

2. Test Methods and Results (Summary) **4**

3. Theory and Evaluation **8**

- 3.0. Formation of solid structure 8
- 3.1. Weight loss and hydration 10
- 3.2. Cracks 14
- 3.3. Chloride penetration 17
- 3.4. Capillary water absorption 19
- 3.5. Carbonation depth 21
- 3.6. Evaluation 25

4. Conclusion **27**

5. Further investigations **29**

List of Literature **30**

List of Symbols **31**

Appendix A: Equivalent W/C, air content and slump of the delivered concrete

Appendix B: The climatic condition during the first 10 Mdays

Appendix C: Weight losses

Appendix D: Micro analysis

Appendix E: Chloride penetration

Appendix F: Capillary water absorption

Appendix G: Carbonation depth

0. Preface

This project regarding curing is part of the Danish Road Directorate's research programme, High Performance Concrete - The Contractor's Technology, in Danish Højkvalitetsbeton - Entreprenørens Teknologi abbreviated to HETEK.

High Performance Concrete is concrete with a service life in excess of 100 years in an aggressive environment.

The research programme includes investigations regarding the contractor's design of high performance concrete and execution of the concrete work with reference to obtain the requested service life of 100 years.

The research programme is divided into eight parts within the following subjects:

- chloride penetration
- frost resistance
- autogenous shrinkage
- control of early-age cracking
- compaction
- curing (evaporation protection)
- trial casting
- repair of defects

The Danish Road Directorate has invited tenders for this research programme which primarily is financed by the Danish Ministry for Business and Industry - The Commission of Development Contracts.

This project regarding curing is performed by:

Danish Technological Institute represented by the Concrete Centre:

- Marlene Haugaard (Head of the project)
- Kirsten Riis
- Tommy Nielsen

and

Danish Concrete Institute represented by the three Contractors:

Højgaard & Schultz A/S - Per Fogh Jensen
Monberg & Thorsen A/S - Jan Graabek
Rasmussen & Schiøtz - Per Jeppesen

The purpose of the project is to investigate the effect of different curing methods on the quality of the concrete surface and to prepare a guideline regarding curing.

Curing method is defined as the combination of the type of surface protection and the protection period.

The results of the project will be published in the following reports:

HETEK - Curing - State of the Art
HETEK - Curing - Supplementary Research - Proposal
HETEK - Curing - Phase 1: Laboratory Tests
HETEK - Curing - Phase 2: Evaluation of Test Results
HETEK - Curing - Phase 3: Verification Tests
HETEK - Curing - Phase 4: Final Evaluation and Definition of Conformity Criteria
HETEK - Curing - Main Report
HETEK - Curing - Guideline.

April 1997
Per Fogh Jensen
Marlene Haugaard
Steering Committee of HETEK-Curing project

1. Introduction

The main issues concerning curing of concrete, are the development of internal structure by the hydration in the concrete and the prevention of failures in the surfaces, which later on are to be exposed to weather conditions (rain, frost, sun), sea water etc. The structure created by hydration lead to density and thereby strength, stiffness, tightness etc.

Experience shows that it is very important, that the concrete is treated properly during the first few days after mixing and casting.

The concrete has to be protected from extreme conditions such as freezing, drying, heating and mechanical deformations, until it is strong enough to withstand such extreme exposures.

To avoid durability failures of concrete structures, it is important to protect the concrete surfaces in such a manner, that the qualities of the surfaces will be as high as wanted.

Desired qualities of the surface normally include properties like high strength, low permeability to water, chloride and carbon dioxide.

In order to fulfill the qualities prescribed in the project, the contractor has to handle problems concerning mixing and transportation of the concrete, form building, casting, curing, surface treatment etc. and he will often be in a position, where contradictory requirements exist.

Surface treatment and requirements to early curing may cause trouble, because the curing sometimes shall be established before the surface treatment has been finished.

The optimum time of demoulding can be contradictory to the required time of curing.

This phase 2 report contains an evaluation of 14 different curing methods performed in the laboratory.

2. Test Methods and Results (summary)

In Phase 1 the effect of fourteen different curing methods have been tested on one type of concrete. This chapter is a short description of the test methods used and a short summary of the results.

For a more detailed description reference should be made to Appendices A-G in this report and to the report HETEK-Curing-Phase 1- Laboratory Tests.

Concrete mix design and casting

The concrete mix design for all the specimens is shown below:

Figure 2.1 Concrete mix design

Recipe no. 6021 from 4K-Beton		
	Type/origin/class	kg/m^3
Cement	Low-alkali Sulfatresistant CEM I 42,5(HS/EA/≤2)	285
Fly ash	Danaske	60
Silica fume	Elkem	12
Water	Water	127
Fine aggregate	RN, Avedøre sand 0/4, SA	758
Coarse aggregate	Rønne granite 8/16, A	535
Coarse aggregate	Rønne granite 16/25, A	565
Air entrainment	Conplast 316 AEA, Fosroc	0.357
Plasticizer	Conplast 212, Fosroc	1.428
Super plasticizer	Peramin F, Fosroc	2.856
Equivalent water-cement ratio (W/(C+ FA · 0,5 + MS · 2)		0.38
Content of FA+MS by weight of C+FA+MS		20.2 %
Content of MS by weight of C+FA+MS		3.4 %

The concrete used for casting the specimens was delivered from a ready-mix plant in Copenhagen. A batch of 3 m^3 was mixed and transported to DTI, Taastrup, where two specimens (550 x 450 mm plates, thickness 100 mm, representing 50 l of concrete) were cast. The transportation time was app. 1 hour. In total 14 specimens were cast.

The equivalent water-cement ratio, the air content and the slump for the delivered concrete are tabulated in *Appendix A*. The equivalent water-cement ratio was stated in the mix report and the air content and slump were tested by DTI at delivery. The specimens were cast on a vibration table except specimens no. 1, 2, 11 and 12 which were cast by means of poker vibrator to avoid air bubbles on the surface.

Curing methods

Immediately after casting the specimen was placed in the evaporation test equipment and cured as described below:

Figure 2.2. Curing methods, survey.

Specimen no.	Plywood Mh	Free surface Mh	Curing compound Mh	10 mm Foam-matt Mh	Wet surface Mh
1	1-76	76-240	-	-	-
2	1-77	77-79	79-240	-	-
3	1-240	-	-	-	-
4	-	2-240	-	-	-
5	1-25	25-240	-	-	-
6	1-25	25-27	27-240	-	-
7	-	1-240	-	-	-
8	1-78	78-80	80-240	-	-
9	-	1-5	5-240	-	-
10	-	2-5	-	-	5-244
11	1-25	25-27	-	27-240	-
12	1-77	77-79	-	79-240	-
13	-	1-5	-	5-240	-
14	-	1-2	2-240	-	-

Below is a short description of the used types of curing.

Plywood: The surface of the specimens were cast against an 18 mm waterproof plywood plate which was placed on the plexiglass-mould. Release agent was used on the plywood plate. The release agent was based on water and ester.

Free surface: No curing was applied.

Curing compound: 234 g/m^2 of curing compound was sprayed on the surface in an even layer. The curing compound was based on water and ester with an efficiency of 84 % according to TI-B 33. The weight loss from the curing compound was tested separately for the first 240 Mh.

Foam Matt: A 10 mm matt of Extruded Ethafoam was placed on the surface. To ensure that the foam-matt was kept close to the surface some weight was placed along the edge.

Wet surface: The wet surface consisted of a sack of hessian which was watered daily.

Evaporation tests

The *evaporation tests* were performed from the time of casting until 10 Mdays. The climate was a temperature of 20 °C and a relative humidity (RH) of 63-68 %. For specimens No. 7 and 8 the relative humidity was 44 %. For specimens no. 1 and 2 the temperature was 22 °C. During periods with free surface and with curing, the wind velocity was 3.6 - 3.7 m/s. The climatic conditions are tabulated as mean values for each specimen in *Appendix B*.

Immediately after casting the specimens were placed on a scale in the wind tunnel and the weight loss was recorded continuously and started as soon as possible.

The specimens for testing curing on a free surface were immediately after casting placed horizontally on the scale in the wind tunnel, so that the surface was exposed to wind from the start.

The specimens for testing mould curing were placed vertically on the scale in the wind tunnel. At the time when the surface of the specimens were demoulded, the specimens were turned to a horizontal position and exposed to wind.

The specimens no. 9, 10 and 13 were cured at 5 Mh which is app. the setting time evaluated from measurement of heat development, where τ_0 is similar to the setting time, see further description in HETEK Control of Early Age Cracking, Phase 1. Early Age Properties of Selected Concrete.

The weight losses are tabulated in *Appendix C*. For the specimens cured with curing compound the weight losses have been compensated for the weight loss of the curing compound. To compare the weight loss from each type of curing the total weight loss is tabulated for each of the 5 different curing types.

For specimens no. 1, 3, 5, 8, 11 and 12 the weight loss was also measured during the period with plywood on the surface. In theory the weight loss in this period should be zero, but in practice there is a weight loss, although it is very small, as it is impossible to make a completely tight mould.

The duration of the evaporation test is app. 10 Mdays. After the evaporation test the specimens were placed in a climate chamber with 20 °C and 65% RH until 28 Mdays. At 28 Mdays samples were cut, as shown in *Appendix A*, from one half of each specimen for testing the quality of the concrete surface. The other half remained in the climate chamber until the samples were cut from all the specimens. Thereafter they were placed outdoors.

Test samples and Test Methods

Figure 2.3. Test specimen, 450 x 550 mm concrete plate, thickness 100 mm.

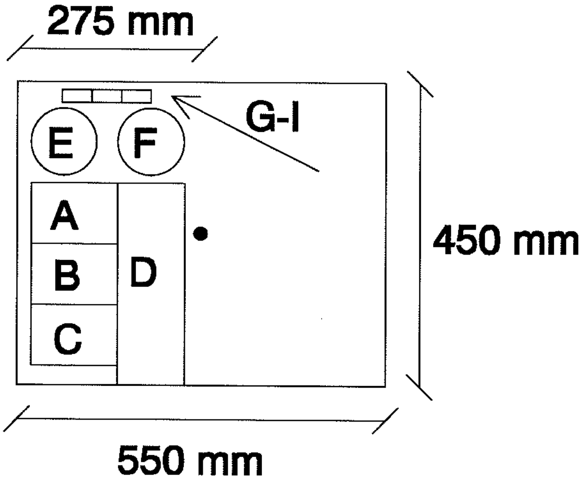

Samples for tests were:

A-C: Capillary water absorption
D: Carbonation
E-F: Chloride penetration
G-I: Micro cracks

Capillary Water Absorption TI-B 25
Three samples, 90 x 130 mm, thickness 30 mm, of each specimen have been tested for absorption of water versus time.

Carbonation NT BUILD 357
One sample, 100 x 100 x 300 mm, of each specimen has been exposed to a concentration of CO_2 at 3.0 % and the carbonation depth was measured 1, 2 and 3 months after start of exposure.

Chloride Penetration AASTHO T 277-83
Two cylinders of each specimen with diameter 100 mm and length 50 mm have been subjected to 60 V(dc) during 6 hours and the electric charge (expressed in Coulombs) passing through the specimen has been recorded.

Micro Cracks TI-B 5 (87)
Three fluorescence impregnated thin sections, 30 x 45 mm, of each specimen have been analysed in microscope for crack number, crack width, crack length and crack orientation. The variation of the porosity was evaluated by studying the variation in water-cement ratio.

3. Theory and Evaluation

3.0 Formation of solid structure

The curing of the concrete must start as soon as possible after casting, to protect the concrete from evaporation, so that the specified degree of hydration can be achieved.

When cement, water, micro silica, fly ash and aggregates are mixed together, a number of chemical processes start. The cement is partly dissolved in the water and the dissolved components react with the solid components and form crystals, that grow in the water filled micro volumes. The crystals grow together very fast in the beginning to form a loosely bound structure of thin crystals, which is not very strong. As time passes the crystals grow and the crystal structure becomes more and more solid, but it never becomes 100% dense. The crystal structure is called gel and it consists of a solid phase of hydrated cement and a water/air phase.

If the initial water content of the fresh concrete is high ($w/c > 0.45$), the reaction products are not able to fill the space between the solid particles, and the concrete will finally contain a lot of microscopic spaces between the gel particles.

On the other hand, if the water content is low ($w/c < 0.45$), the reaction between water and solid materials will stop, when all the water has reacted with the cement. The result is in principle the same as in the situation, where the water content is high. The reaction will stop before the products are able to fill the spaces between the solid particles totally. The result is that microscopic air gaps are included in the gel.

In the first case (high water content) the air gaps are water filled, and in the second case (low water content) the gaps are air filled.

Since the hydration process normally leaves pores in the gel material, the concrete is never 100 % dense. It will always have a porosity of a finite magnitude.

At the time when the concrete is mixed, the initial porosity p_0 in the paste is determined by the water-cement ratio (Powers [1948]):

$$p_0 = 1 - 1/(1 + 2.92 \cdot W/C_e)$$

where the equivalent cement content C_e is defined as

$$C_e = C + 0.5 \cdot FA + 2 \cdot MS$$

where

C = cement content
FA = fly ash
MS = micro silica

and the number 2.92 represents the avarage density of C + FA + MS.

The capillary water content in the cement paste by volume V_{cap} can be determined as a function of the degree of hydration (ß) and the initial porosity of the cement paste (p_0) by the equation (ref.: Hansen [1978]):

$$V_{cap} = p_0 - 1.4 \bullet (1 - p_0) \bullet \text{ß}$$

If evaporation by an amount dW takes place, V_{cap} is reduced accordingly:

$$V_{cap} = p_0 - 1.4 \bullet (1 - p_0) \bullet \text{ß} - dW$$

From this equation can be found the value of ß, that corresponds to the final state, where no capillary water is left for the hydration process, $V_{cap=0}$:

$$\text{ß} = (p_0 - dW) / (1.4 \bullet (1 - p_0))$$

(dW = dU / 24.2, where dU is water loss in kg/m², concrete thickness = 0.1 m, volume fraction of paste in concrete = 0.242).

Figure 3.0.1: Porosity of cement paste during hydration as a function of degree of hydration.

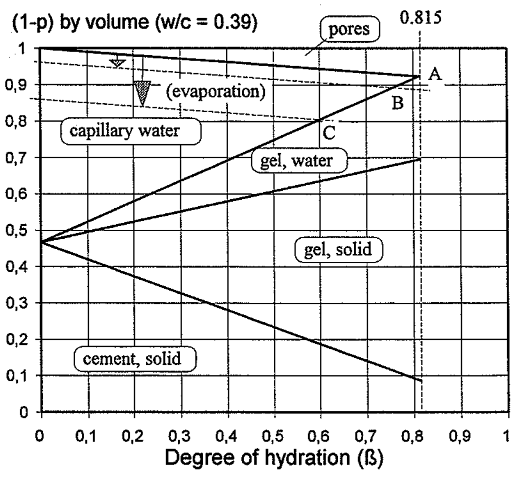

By substitution the following equation is found to calculate $V_{cap=0}$ as a function of the initial W/C_e and the water loss dU during hydration:

$$V_{cap=0} = 0.857 + 0.143 / (1 + 2.29 \bullet W/C_e) - 0.0354 \bullet dU$$

V is the density of the cement paste by volume. Index cap = 0 indicates the density which can be obtained, when the capillary water content becomes zero.

The coefficents in the formula are only valid in the concrete used in the project at a thickness of 100 mm

In *Figure 3.0.1* lines are drawn that correspond to $W/C_e = 0.39$ (W/C_e of the specimens in the project range from 0.37 to 0.39, but as 0.39 is the most frequent value, it is used in this figure). It is obvious, that the capillary water content becomes zero, when the theoretical degree of hydration ß (equivalent to the degree of hydration of the cement) obtains the value 0.815. The maximum degree of hydration $ß_{max}$ has the value $ß_{max}=1$ when the point A is reached. So the following relation exists:

$$ß_{max} = ß / 0.815$$

If evaporation takes place before the point A has been reached, there will not be a sufficient amount of water left for the concrete to reach the point A. In *Figure 3.0.1* are shown two dotted lines representing two levels of reductions in the capillary water content caused by evaporation from the concrete. It is obvious that the concrete can only reach the points B or C, depending on the amount of evaporation. The lower dotted line represents the level of evaporation that has been measured from specimens 4 and 7.

Below (section 3.1) the values of $V_{cap=0}$ are calculated for each of the fourteen specimens and used as a parameter that represents the porosity of the structure formed in the concrete.

The basic hypothesis is that parameters like crack formation, chloride penetration rate, capillary suction and carbonation depth depend on the structure density of the cement paste, $V_{cap=0}$.

This hypothesis forms the theoretical background of the requirements for maximum evaporation of water prior to protection against drying out and the earliest time for removal of protection against drying out as they are described in "Almindelig arbejdsbeskrivelse" (AAB) [Vejregeludvalget, 1994] and "Basisbetonbeskrivelse" (BBB) [ATV-udvalget vedr. betonbygværkers holdbarhed, 1987].

Caused by the fact that V_{cap} is a function of the degree of hydration (β) as described at page 13 the requirements concerning the earliest time for removal of the curing are formulated as requirements to the minimum degree of reaction depending on the actual environmental class of the construction.

In the following sections (3.2 - 3.5) this hypothesis is investigated.

A few alternative hypotheses have been considered. An example of such a hypothesis is to say, that a big loss of water by evaporation will produce cracks in the concrete and so reduce its structural density and resistance to chloride penetration and to carbonation. However, with the available results from this project in mind, these kinds of hypotheses have been rejected, and only the hypothesis mentioned

3.1 Weight loss and hydration

As described in the previous chapter, 14 concrete specimens have been cast and subjected to various curing regimes in order to study the effect of different curing methods on the concrete.

Evaporation from the specimens during the first 10 Mdays after casting, determined as weight losses, have been recorded continuously. During the following period from 10 Mdays to 28 Mdays the specimens were kept in a climate chamber at 20 °C and 65 % RH. The weight losses during this period were not recorded. The weight losses are evaluated to be a minimum.

In *Figure 3.1.1* four graphs of weight loss versus time are shown representing the following curing conditions:

Specimen no. 4: Free surface
Specimen no. 5: Mould in 1 Mday
Specimen no. 6: Mould in 1 Mday + Curing compound
Specimen no. 1: Mould in 3 Mdays

Figure 3.1.1: Weight loss of typical specimens versus time

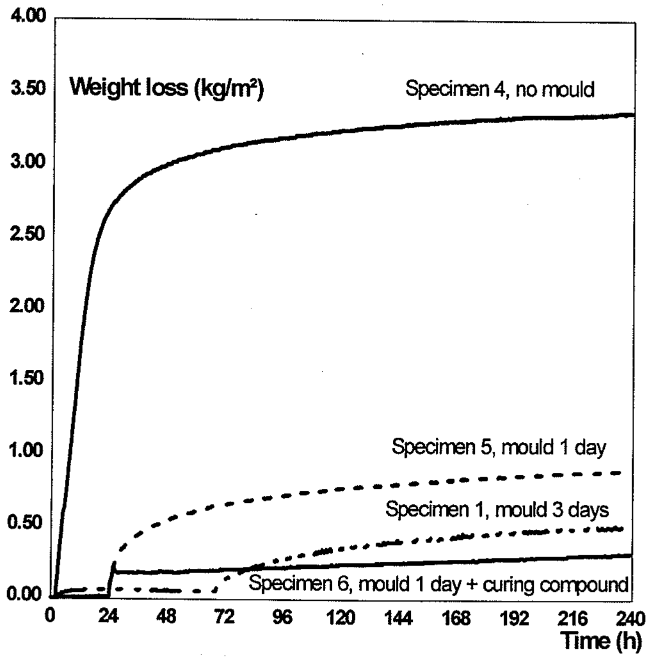

The initial weight loss for the specimen with free surface (specimen 4) are about 170 g/m²h during the first 12 Mh. During the first 12 Mh the temperature is lower in the concrete than in the air, because it is cooled by the evaporation process. The temperature is about 16°C in the concrete and 20°C / 60 % RH in the air. With these values a theoretical calculation, based on the guidelines given in the State of the Art Report, gives an evaporation rate ~200 g/m²h, which is in good agreement with the measured values.

The weight loss for specimens protected with curing compound or foam-matt after demoulding (specimen 6 in Figure 3.1.1) included a short period after demoulding with very intense evaporation (~ 200 g/m²h), during which a significant part of the total water loss took place. After the curing was applied, the evaporation rate dropped to an almost constant and very low rate.

In *Figure 3.1.2* the measured values of total weight loss at 10 Mdays are tabulated in ascending order of weight loss. The corresponding values of $V_{cap=0}$ calculated as described above are also listed. The negative values of specimen no. 10 represent a raise in weight during water curing.

Figure 3.1.2. Total measured weight loss (dU) and calculated structure density parameter ($V_{cap=0}$) by specimen no. sorted in ascending order of dU.

Spec.- No.	dU (kg/m²)	$V_{cap=0}$ (m³/m³)	$ß_{max}$	Curing method
10	-0.67	0.948	1.05	Water cured
3	0.04	0.923	1.00	Mould in 10 Mdays
12	0.08	0.921	0.99	Mould in 3 Mdays + Foam-matt
2	0.22	0.918	0.98	Mould in 3 Mdays + Curing compound
8	0.23	0.917	0.98	Mould in 3 Mdays + Curing comp. - 44% RF
11	0.27	0.914	0.98	Mould in 1 Mday + Foam-matt
6	0.32	0.914	0.98	Mould in 1 Mday + Curing compound
14	0.34	0.912	0.97	Curing compound after 2 Mh
1	0.51	0.908	0.96	Mould in 3 Mdays
13	0.66	0.901	0.95	Foam-matt after 5 Mh
5	0.91	0.893	0.93	Mould in 1 Mday
9	1.14	0.884	0.91	Curing compound after 5 Mh
4	3.39	0.804	0.74	Free surface
7	3.56	0.799	0.72	Free surface - 44% RF

In figure 3.1.3 the measured total weight losses are shown as a function of the structure parameter $V_{cap=0} = 0.857 + 0.143 / (1 + 2.29 \cdot W/C_e) - 0.0354 \cdot dU$ as described in section 3.0.

Figure 3.1.3. Total weight loss during curing (10 Mdays) versus structure density parameter $V_{cap=0}$.

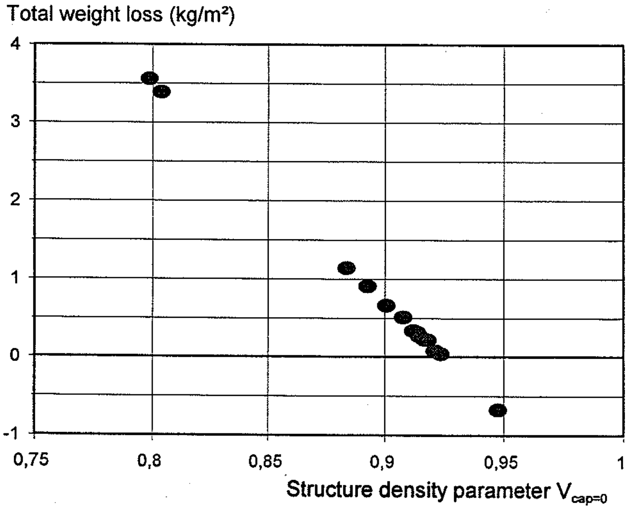

The graph shows that the water loss has the major influence on the structure parameter, and influences of variations in W/C_e are very small (all points are almost on a straight line with the slope -1/0.0354). This is of course partly caused by the fact that in this project W/C_e varies very little (0.37-0.39).

In the part project HETEK-4 the heat development as a function of the maturity for the concrete investigated in this project has been measured. From this measurement the degrees of hydration corresponding to 1, 3, 5, 7 and 10 Mdays have been evaluated, see HETEK-Curing-Guideline. In *Figure 3.1.4* these values are shown in an expanded version of *Figure 3.0.1,* and curves have been drawn, that represent the time dependent loss of water for typical specimens.

It can be seen that only specimens 4 and 7 end in point C. All other specimens end in points between the points A and B (except specimen 10, water cured, which end in a point above point A) .

Figure 3.1.4: Porosity of cement paste during hydration as a function of degree of hydration (ref. Figure 3.0.1). The smooth curves indicate the loss of water in the specimens. Only two specimens end in point C, while the rest of the specimens end in points above point B.

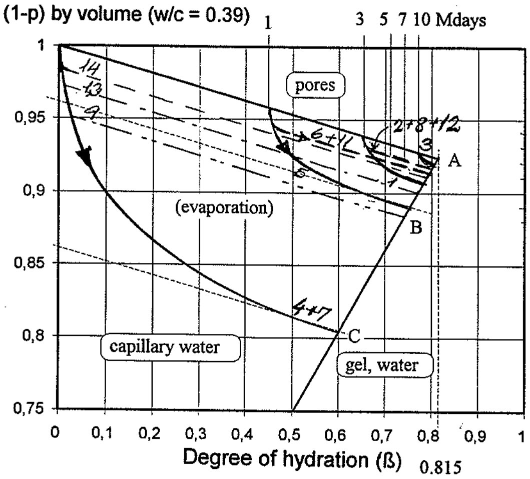

The decrease in theoretical structure formation caused by water loss may be used to divide the specimens into three groups:
- Specimen 10 (no water loss) with the most dense structure.
- Specimens no 4 and 7 (maximum possible water loss) with the less dense structure
- The rest of the specimens.

In figure 3.1.4 is shown that even specimen no. 5, mould in 1 Mday has the possibility to reach a degree of hydration $\beta_{max} = 0{,}93$. The degree of hydration at the time of de-moulding is $\beta_{max} = 0{,}56$.

3.2 Cracks

Generally cracks in concrete are assumed to reduce the durability, because cracks represent weaknesses in the structure.

The presence of cracks in a solid structure like concrete might be expected to increase the transport abilities of liquid and gaseous components like water, chloride ions and carbon dioxide. This is obvious the case when talking about liquids passing in the direction of the cracks, the phenomenon known as capillary suction, which takes place at high water contents, where RH ~ 100 %.

When the influence of cracks on transport phenomena perpendicular to the concrete surface is studied, the direction of the cracks must be considered. Cracks perpendicular to the surface might promote transport and cracks parallel to the surface might represent obstacles to the transport.

One problem is, that cracks are measured in a plane section perpendicular to the surface. If the cracks theoretically are assumed to be represented by plane surfaces located randomly in the spatial structure, they will be seen as lines in a plane section. But such a line, which appears to be parallel to the surface, might represent a crack plane, which is almost perpendicular to the concrete surface and at the same time almost parallel to the section plane. This demonstrates, that when counting cracks in a plane section perpendicular to the surface, cracks parallel to the surface are overestimated in relation to cracks perpendicular to the surface. Generally the spatial angle between a crack plane and the surface plane will be estimated into an angle, which is more parallel to the concrete surface.

Another problem is, that the effect of cracks on transport properties also depends on the width, and thereby on the volume, of the cracks. So when the total relative volume of the cracks is very small, their influence on transport processes like electrical conduction of chloride ions, water suction, CO_2 diffusion etc. must also be very small.

In the test method used in this project thin sections of the concrete have been produced by cutting, impregnating and grinding the concrete, so that a thin slice of the concrete is left, fastened on a glass plate. This thin section is studied under microscope.

In the test method is distinguished between three categories of surface cracks:

> *Micro cracks (width < 0.01 mm), fine cracks (0.01 mm < width < 0.1 mm)* and *coarse cracks (0.1 mm < width)*

and between two categories of crack angles:

> *Cracks perpendicular to surface* and *parallel to surface*:

Furthermore, the test method distinguishes between two categories of cracks:

> *Paste cracks* and *adhesion cracks and defects*

The test reports present countings of 8 combinations of categories of cracks:

Surface (outmost 2.5 mm, area analysed ~ 100 mm²):
1. Micro cracks, perpendicular to surface
2. Micro cracks, parallel to surface
3. Fine cracks, perpendicular to surface
4. Fine cracks, parallel to surface
5. Coarse cracks, perpendicular to surface
6. Coarse cracks, parallel to surface

Internal structure (area analysed ~ 60 mm²):

7. Paste cracks
8. Adhesion cracks and defects

Furthermore the length of each crack in the surface was recorded.

An essential result was, that no coarse cracks (type 5 and 6) were found in any of the 14 specimens.

Each of the parameters 1-8 has been investigated for correlation between the crack parameter and the structure density parameter $V_{cap=0}$, but no or only weak correlations could be found. As indicated in the arguments above, possible effects of cracks on transport phenomena depend on the volume or the length of the cracks, and therefore and in order to include as much information as possible from the measurements to rank the concretes, the following has been done for each specimen:

- The length of all cracks (the types 1, 2, 3 and 4) in the surface layer has been calculated as an average by specimen.
- The number of paste cracks in the internal structure was calculated as an average pr m² by specimen.

The results are tabulated in *Figure 3.2.1*.

Figure 3.2.1. Length of cracks in surface (outermost 2.5 mm) and number of paste cracks, ranked by the length of surface cracks

Sp. no.	Surf. (mm)	Paste (no/mm²)	Curing method
7	0.0	0.02	Free surface - 44% RF
5	1.2	0.06	Mould in 1 Mday
8	1.4	0.09	Mould in 3 Mdays + Cur.comp. - 44% RF
4	2.9	0.01	Free surface
14	4.6	0.04	Curing compound after 2 Mh
11	5.2	0.04	Mould in 1 Mday + Foam-matt
2	7.4	0.27	Mould in 3 Mdays + Cur. comp.
6	7.7	0.15	Mould in 1 Mday + Curing compound
12	8.8	0.09	Mould in 3 Mdays + Foam-matt
13	10.1	0.18	Foam-matt after 5 Mh
1	12.3	0.29	Mould in 3 Mdays
9	15.5	0.06	Curing compound after 5 Mh
3	16.4	0.12	Mould in 10 Mdays
10	17.7	0.30	Water cured

To see if there is any correlation between the structure parameter $V_{cap=0}$ and the cracks measured in this section, two graphs have been made, *figure 3.2.2 and 3.2.3*, where the two crack parameters listed in *figure 3.2.1* are drawn versus the structure parameter.

Figure 3.2.2. Length of surface cracks (total area analysed: 3 x 100 mm²) versus structure density parameter $V_{cap=0}$

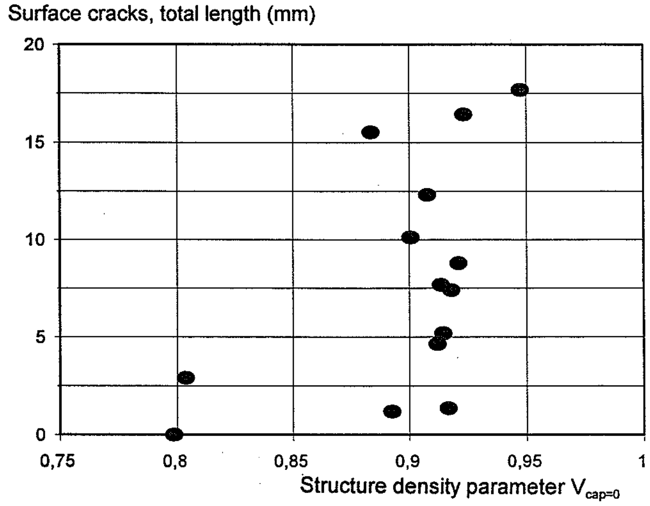

Figure 3.2.3. Number of paste cracks in internal structure (area analysed: 60 mm²) versus structure density parameter $V_{cap=0}$

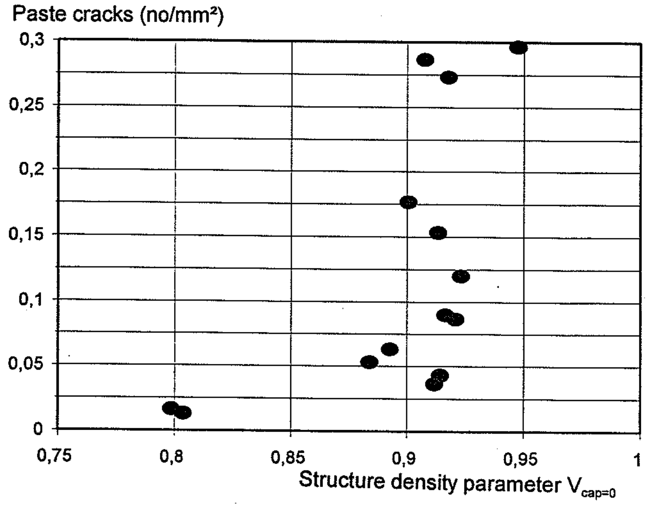

The two figures 3.2.2 and 3.2.3 show that the general tendency to form cracks increases with the structure density of the concrete, although the correlation between cracks formation and structure density is very weak.

This is contradictory to the expectations that an increased amount of cracks lead to a less dense structure. The increased amount of cracks can be explained by the following: Internal stresses in the cement paste will arise due to the hydration of the cement. The less water is evaporated from the concrete, the more water will react with the cement, and the amount of cracks will increase due to the formation of stresses. This is only correct when the water/cement ratio is less than 0.45 according to Powers.

3.3 Chloride penetration

Penetration of chloride into reinforced concrete is harmful, because chloride is able to attack the reinforcement.

In the chloride penetration test used in this project the electrical conductance of concrete is measured in order to give a rapid indication of its resistance to the penetration of chloride ions. The total charge passing through the cylinder was used to rate the concrete's permeability to chloride ions.

The results of the measurements are tabulated in *figure 3.3.1*. The results have been ranked in ascending order of chloride penetration rate.

Figure 3.3.1. Specimen no. versus values of chloride penetration (Coulombs), sorted in ascending order of chloride penetration.

Speci-men	Chloride pen. (Coulombs)	Curing method
8	951	Mould in 3 Mdays + Curing comp. - 44% RF
10	985	Water cured
14	985	Curing compound after 2 Mh
1	1013	Mould in 3 Mdays
2	1049	Mould in 3 Mdays + Curing compound
12	1059	Mould in 3 Mdays + Foam-matt
11	1084	Mould in 1 Mday + Foam-matt
13	1463	Foam-matt after 5 Mh
6	1556	Mould in 1 Mday + Curing compound
9	1710	Curing compound after 5 Mh
5	1717	Mould in 1 Mday
3	2139	Mould in 10 Mdays
4	>4000	Free surface
7	>4000	Free surface - 44% RF

The measured values of chloride ion penetrations have been plotted versus the structure parameter (see section 3.1) in *figure 3.3.2*. Specimens no. 4 and 7 have been plotted with the value 4000 coulombs, although the measurements only state that the values are higher than 4000 coulombs.

Figure 3.3.2. Chloride penetration versus structure density parameter $V_{cap=0}$. The points plotted with the value 4000 should really be >4000.

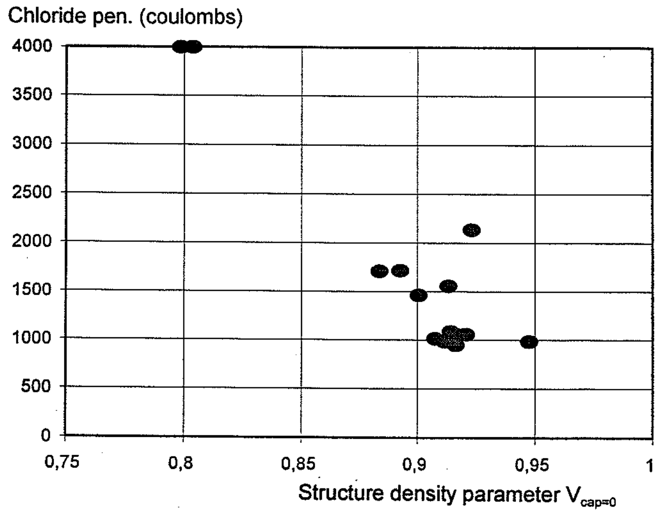

The figure shows a distinct correlation between structure density and chloride penetration (coulombs). This is in good agreement with expectation, that a less dense structure should allow more chloride ions to pass through.

3.4 Capillary Water Absorption

When a dry concrete surface is subjected to water, some water is absorbed in the concrete, until it eventually enters a state of equilibrium. The ability of the concrete to absorb water is a function of its internal structure, and has been tested in this project as follows:

Samples, area 90 x 130 mm, 30 mm thick, were cut from the concrete so that the surface to be tested was included *(see appendix B).*

The samples were dried for a week in an oven at 50 °C and then placed with the surface under test facing down on a water surface during (more than) 10 days. The samples were weighed before and regularly during the exposure to water. Afterwards the samples were dried in an oven at 105 °C until constant weight, filled with water using vacuum and then weighed under water to calculate the volume.

The degree of filling was calculated and plotted versus the square root of time.

The test method prescribes to find the point where the graph changes from a sloping line into a (almost) horizontal line by intersecting two tangents (placed at the start and at the end of the measurement period).

The results of this method are difficult to interpret, because in many measurements, the curves do not change abruptly from a sloping line into a horizontal line. Instead of two straight lines the measurements often yield graphs that change smoothly from an initial slope to almost horizontal. This is demonstrated in *figure 3.4.1,* where all measured values are plotted together.

Figure 3.4.1. Measurements of degrees of saturation versus time (square root of hours). All 14 specimens are shown together.

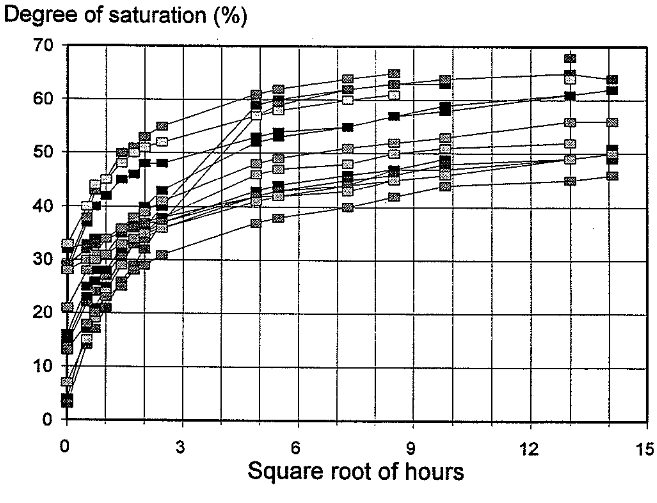

In order to try to find an alternative way to interpret the results, the square root of time model has been tested on the measurements performed in this project by plotting all results in a log-log graph. If the capillary suctions could be represented by straight lines in the square root of time model, all measurements would yield straight lines with slope 0.5 (decades per decade) in a log-log graph. The result was that the graphs had slopes in the range 0.2 - 0.5 (decades per decade), and so this experiment was abandoned.

The graphs have been interpreted in the prescribed manner to give values of Q_{cap} and t_{cap}, which are the coordinates of the points of intersection mentioned above.

As Q_{cap} represents the degree of water saturation, it is relevant for evaluating frost resistance. The lower Q_{cap} is, the higher the frost resistance is.

As high values of t_{cap} represent high resistance to penetration by water, it should also be expected to represent high resistance to chloride ions penetration.

Investigations showed very low correlations between each of these two parameters Q_{cap} and t_{cap} and the structure density parameter $V_{cap=0}$.

In order to evaluate a combination of these two qualities, the following expression has been used (the factor 0.1 is used to give the two parameters Q_{cap} and t_{cap} the same weight).

$$\text{Cap} = 0.1 \bullet Q_{cap} + t_{cap}$$

In *figure 3.4.2* the values of Cap are tabulated versus specimen number and sorted in order of descending values of Cap.

Figure 3.4.2. Specimen no. versus values of Q_{cap} and t_{cap} sorted in descending order of Cap

Spec. No.	Q_{cap} (%)	t_{cap} ($h^{0.5}$)	Cap	Curing method
2	61	5.3	11.4	Mould in 3 Mdays + Curing compound
1	61	5.0	11.1	Mould in 3 Mdays
11	60	3.4	9.4	Mould in 1 Mday + Foam-matt
14	42	4.4	8.6	Curing compound after 2 Mh
3	52	3.3	8.5	Mould in 10 Mdays
8	43	4.1	8.4	Mould in 3 Mdays + Curing comp. - 44% RF
13	49	3.1	8.0	Foam-matt after 5 Mh
12	56	2.1	7.7	Mould in 3 Mdays + Foam-matt
10	51	2.6	7.7	Water cured
7	38	3.4	7.2	Free surface - 44% RF
4	46	2.3	6.9	Free surface
9	41	2.8	6.9	Curing compound after 5 Mh
6	41	2.4	6.5	Mould in 1 Mday + Curing compound
5	40	2.2	6.2	Mould in 1 Mday

Figure 3.4.3. Capillary parameter Cap = 0.1 • Q_{cap} + t_{cap} versus structure density parameter $V_{cap=0}$

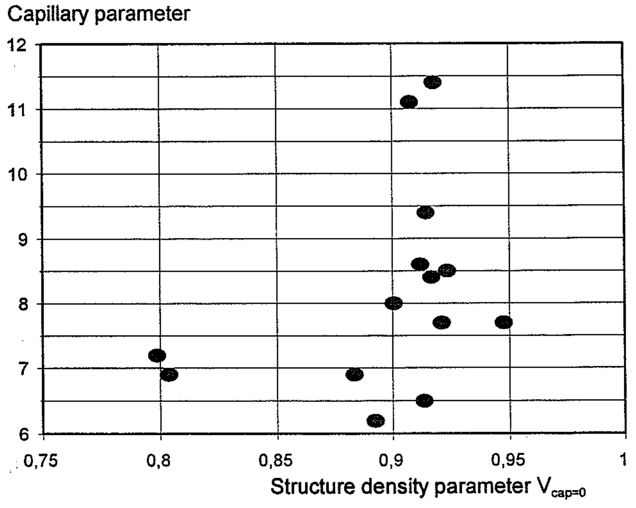

In *figure 3.4.3* the parameter Cap has been graphed versus the structure parameter $V_{cap=0}$. The figure shows that no correlation exist between $V_{cap=0}$ and Cap. Therefore the conclusion must be that no correlation has been found between the structure density parameter $V_{cap=0}$ and the capillary suction process.

3.5 Carbonation depth

The velocity of the carbonation process in concrete is of high importance. The carbonation starts at the surface and develops into the concrete. When the carbonation reaches the reinforcement, the chemical protection of the reinforcement from the concrete stops and the reinforcement starts to corrode.

The velocity of the carbonation process is described by Bentur and Jaegermann [Bentur, 1991] with the depth as a function of time raised to the power 0.4. They also found that the velocity of carbonation in accelerated tests (CO_2 content = 5 %) was 7.5 times higher than that in natural air. When the CO_2 content of natural air is assumed to be 0.03 %, it is found, that if a power model is used to forecast values measured in accelerated tests, i.e. $(5/0.03)^x = 7.5$, the value of the power x to fit this model is 0.38.

As the power 0.38 is close to the power 0.4, the indication is that the Bentur and Jaegermann model is well suited to describe the carbonation process, if values measured in accelerated tests are multiplied by $[CO_2]$ / 0.03, where $[CO_2]$ represents the CO_2 concentration used in the test, and 0.03 is the natural concentration of CO_2.

Figure 3.5.1 Depth of carbonation versus age. The graphs labelled "HETEK 6" are those measured in this project (1, 2 and 3 months accelerated test in 3% CO_2). The two graphs labelled "Nagathi et al." represent measurements in laboratory air.

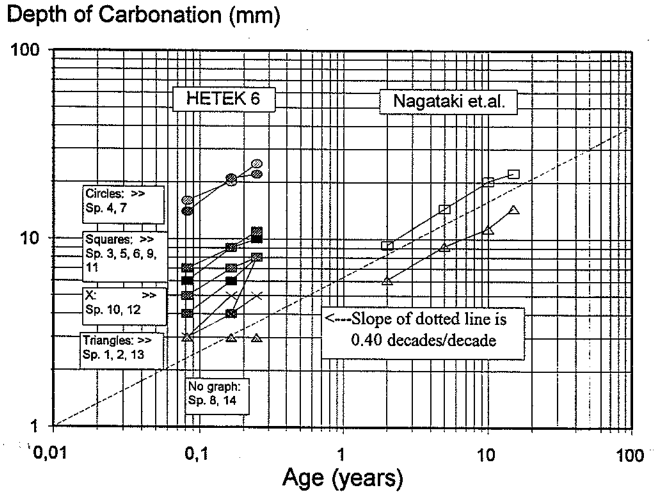

To verify this model, the measurements made in this project have been shown in a log-log-graph together with two series of measurements made by Nagataki et al., see *figure 3.5.1*. The two series represent the following conditions:

Series 1. C+FA = 290 kg/m3, FA/(FA+C) = 0,
air content 2.1 %, initial curing 7 days in water, indoor curing.
Series 2. Same as 1. yet FA/(FA+C) = 30 and air content 1.8 %

In *figure 3.5.1* has been drawn a line with the slope 0.4 (decades/decade). It is seen from the graphs, that most of the measurements made in this project as well as the two measurements made by Nagataki et al. have slopes close to 0.4.

In order to convert the accelerated tests in this project (tested with CO_2 concentration 3.0%) into equivalent real lifetime tests made with natural CO_2 content (0.03%), the time scale must be multiplied by a factor 3.0/0.03 = 100. The result is shown in *figure 3.5.2*. It is seen that the two worst-case specimens 4 and 7 would reach 20 mm carbonation depth after about 15 years of exposure to natural CO_2 content.

Figure 3.5.2 Depth of carbonation versus age. This figure shows the same measurements as Figure 3.5.1, but in this figure the graphs labelled "HETEK 6" are shifted to the right by a factor 100 corresponding to the concentration in the accelerated test.

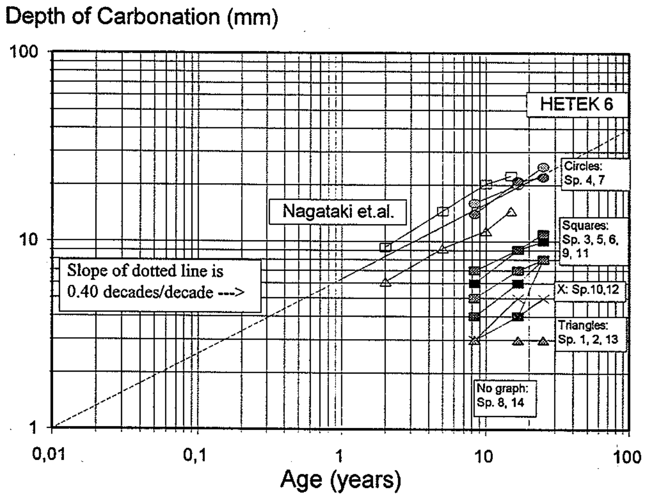

The specimens with the lowest values of carbonation measured (specimens 8 and 14) would reach less than 10 mm carbonation depth after 100 years exposure to natural CO_2 content.

In order to rank the test results in this project the following steps have been used:

1. All measured penetration depths have been extrapolated one by one to 100 years using the log-log model with slope 0.4 mentioned above. Test results with no measured penetration depth were disregarded.
2. For each specimen the averages of the d_k and the d_{max} values were calculated.
3. The specimens were ranked according to d_k.

The result was as follows:

Figure 3.5.3. Specimens listed after equivalent carbonation depth (d_k) (equivalent to average carbonation depth after 100 years, assuming natural CO_2 content)

Speci-men no.	Eq. carb.depth (mm)		Curing method
	d_k	d_{max}	
14	0	4.1	Curing compound after 2 Mh
8	0	5.2	Mould in 3 Mdays + Curing comp. - 44% RF
2	5.7	7.4	Mould in 3 Mdays + Curing compound
1	5.7	8.4	Mould in 3 Mdays
13	6.5	9.6	Foam-matt after 5 Mh
12	8.3	14.7	Mould in 3 Mdays + Foam-matt
10	9.0	16.1	Water cured
9	11.0	15.3	Curing compound after 5 Mh
6	12.3	15.2	Mould in 1 Mday + Curing compound
11	13.9	19.6	Mould in 1 Mday + Foam-matt
3	17.4	21.9	Mould in 10 Mdays
5	18.8	22.3	Mould in 1 Mday
7	39.7	46.9	Free surface - 44% RF
4	42.6	47.9	Free surface

The equivalent carbonation depth has been plotted versus the structure parameter V_{c+g} in *figure 3.5.4.*

Figure 3.5.4. Values of carbonation depths, forecasted to 100 years, versus structure density parameter $V_{cap=0}$. The forecast is based on a concentration factor on the time scale and a log-log time dependence with a slope of 0.4 (decades/decade).

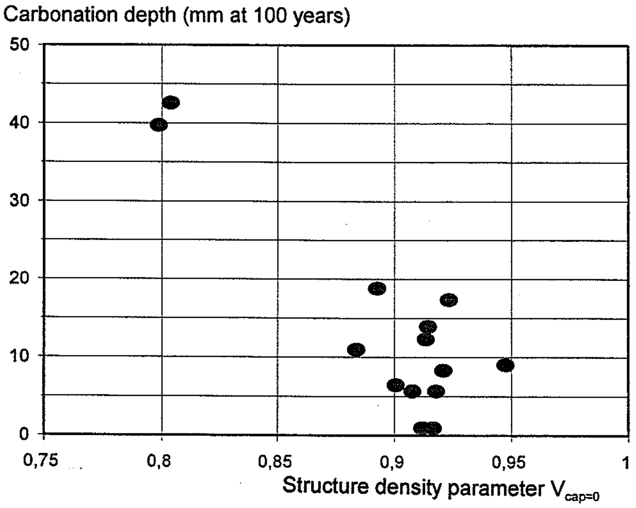

Figure 3.5.4 shows a general correlation between the structure density parameter $V_{cap=0}$ and carbonation depth. This is in good agreement with what may be assumed: That a less dense structure allows more carbonation than a more dense structure.

3.6 Evaluation

The total quality of the surface of the specimens have been rated in the following manner:

The range of values of $V_{cap=0}$ and each of the four measured parameters (crack formation, chloride penetration, capillary suction and carbonation) have been normalised into the range 0-100. (The crack formation parameter is calculated as the average value of the parameters calculated from the surface cracks and the paste cracks).

With the normalised values a linear regression analysis has been performed on each of the four parameters as a function of the structure density parameter $V_{cap=0}$. The results are given below:

Figure 3.6.1 Results of regression analysis

Test	Correlation coefficient	Slope
3.2 (cracks)	0.38	0.64
3.3 (chloride pen.)	0.86	-1.10
3.4 (cap. suct.)	0.13	0.38
3.5 (carbonation)	0.76	-0.90

The four normalised parameters have been weighted with the slope and added together to form a Weighted Sum Parameter called WSP.

As an example SWP for specimen 1 is calculated as follows:

$$WSP_1 = 0{,}64 \cdot 83 - 1{,}10 \cdot 2 + 0{,}38 \cdot 94 - 0{,}90 \cdot 13 = 75$$

Figure 3.6.2. Summary of measurements, normalised parameters (range 0 - 100) (WSP = weighted sum of parameters)

Test no.	$V_{cap=0}$	Cracks	Chloride pen.	Capillary abs.	Carbonation	WSP
1	73	83	2	94	13	75
2	80	66	3	100	13	65
3	84	66	39	44	40	-20
4	4	10	100	13	99	-187
5	63	14	25	0	44	-58
6	77	47	20	6	29	-15
7	1	3	100	19	92	-184
8	79	19	0	42	2	26
9	57	53	25	13	26	-11
10	100	99	1	29	21	54
11	78	22	4	62	32	3
12	82	39	4	29	19	15
13	68	58	17	35	15	18
14	76	19	1	46	2	27

Figure 3.6.3. Specimen no. and curing methods ranked in descending order of WSP*. β_{max} represent the degree of hydration which is obtainable at the actual water loss.

Spec. no.	WSP*	β_{max}	Curing method
1	75	0.96	Mould in 3 Mdays
2	65	0.98	Mould in 3 Mdays + Curing compound
10	55	1.05	Water cured
14	27	0.97	Curing compound after 2 Mh
8	26	0.98	Mould in 3 Mdays + Curing comp. - 44% RF
13	18	0.95	Foam-matt after 5 Mh
12	15	0.99	Mould in 3 Mdays + Foam-matt
11	3	0.98	Mould in 1 Mday + Foam-matt
9	-11	0.91	Curing compound after 5 Mh
6	-15	0.98	Mould in 1 Mday + Curing compound
3	-20	1.00	Mould in 10 Mdays
5	-58	0.93	Mould in 1 Mday
7	-184	0.72	Free surface - 44% RF
4	-187	0.74	Free surface

Note: WSP*: Weighted sum of normalised, measured parameters.

4. Conclusion

The basic hypothesis, as described in section 3.0, is that parameters like crack formation, chloride penetration rate, capillary suction and carbonation depth depend on $V_{cap=0}$.

A theoretically calculated parameter (structure density parameter $V_{cap=0}$) has been used to describe the final cement paste density, that can be obtained as a function of initial W/C_e ratio and the amount of water evaporated until 10 Mdays after casting.

Four parameters have been measured to evaluate the effect of the various curing methods. From the results the following conclusions can be drawn:

- No correlation has been found between the structure density parameter $V_{cap=0}$ and parameters used to describe capillary suction.
- Only weak correlation has been found between structure density parameter $V_{cap=0}$ and the formation of cracks in the surface (2.5 mm) and in the cement paste.
- A correlation has been found between structure density parameter $V_{cap=0}$ and chloride penetration.
- A correlation has been found between structure density parameter $V_{cap=0}$ and carbonation depth.

Each of these parameters has been correlated to the structure density parameter $V_{cap=0}$. A weighted sum of the four parameters capillary suction, cracks, chloride penetration and carbonation depth has been calculated and used to rank the curing tests. Based on this ranking the following grouping of the curing methods can be made:

- The following methods are ranked with the highest values of the weighted sum of parameters:
  - Mould in 3 Mdays, with or without curing afterwards
  - Water curing
  - Curing compound after 2 Mh
  - Foam-matt after 5 Mh
- The following methods are ranked with average values of the weighted sum of parameters:
  - Curing compound after 5 Mh
  - Mould in 1 Mday, with or without curing afterwards
  - Mould in 10 Mdays
- The following methods are ranked with low values of the weighted sum of parameters:
  - Free surface

For the methods with mould in 1 or 3 Mdays no significant effect of additional use of curing compound or Foam-matt after demoulding has been found.

The result of this phase of the project is, that the hypothesis has been confirmed for class A concrete with fly ash and micro silica and with a equivalent water/cement ratio of 0.38.

Three remarkable achievements are:

1. Curing with curing compound after 2 Mh has given good results.
2. Curing in mould in 10 Mdays has obtained a low rating.
3. Only low values of crack formation have been obtained in specimens without curing (free surface).

If these results can be shown to be general, some reductions in the specifications should be the result with regard to curing, but further investigations are necessary to confirm the results.

The remarkable result with curing compound after 2 Mh must be investigated further in a test series with different curing types and concrete types before it can be common procedure for the contractor. The results with curing in mould in 10 Mdays confirms a previous result, reported in [Lundberg, 1994], and must lead to a less restricted requirement in the AAB to the total curing time.

It must be emphasised, that the low values of crack formation in concretes without curing (with free surface), are in accordance with theoretical considerations saying that the micro cracks in concretes with low water/cement ratios (w/c < 0.45) are a result of the hydration process. This means, that few cracks should be expected, when the hydration process is slowed down because of drying out of the concrete surface. If no micro cracks are found in the surface of concrete with low w/c ratio, it may indicate that the concrete has not been cured properly.

The overall conclusion of this investigation is that the concrete surface must be protected against evaporation to secure a proper dense cover of the concrete. The investigation also seems to confess the ordinary requirements in AAB, where the duration of curing for concrete constructions in aggressive and extra aggressive environment shall be performed in a period resulting in a degree of reaction based on the adiabatic heat development of more than 85 - 90%.

5. Further investigations

In phase 3 of the project HETEK 6 - Curing, the tests performed in phase 1 and evaluated in phase 2, are verified by performing further tests.

The verification include four curing methods tested in DTI's laboratory and six curing methods tested in the field.

The first two curing tests are performed with the same concrete mix design as in phase 1. The other two curing tests are performed with the same concrete mix design as in the field tests. All four laboratory tests are performed under controlled climatic conditions, with the same procedures as in phase 1.

The tests in the field are performed on a bridge construction. To monitor the actual climatic condition during the tests, a weather station is placed close to the tested concrete surface.

Samples are cut from all the test specimens. The crack formation in the surface, the chloride penetration rate, the capillary water absorption and the carbonation depth are tested.

The results are verified in phase 4 of the HETEK 6 - Curing project.

List of Literature

Bentur, A. and Jaegermann, C.: "Effect of curing and composition on the properties of the outer skin of concrete". Journal of materials in civil engineering, Nov.. 1991. pp 252-262.

Hansen, P. Freiesleben: Hærdeteknologi-1. Aalborg Portland & BKF-Centralen. 1978.

Justesen: Beton-Teknik 3/11/1982.

Nagataki, Ohga and Kim: "Effect of curing conditions on the carbonation of concrete with fly ash and the corrosion of reinforcement in long-term tests". ACI publication, 1986. pp. 521-540.

Powers, T.C. and Brownyard, T.L.: "Studies of the Physical Properties of Hardened Portland Cement Paste". Portland Cement Association. Chicago 1948. Pp. 101-992. Series: PCA Research Department Bulletin 22.

Berrig, A. & Haugaard, M. & Fogh Jensen, P.: "HETEK - Curing - State of the Art", report No. 37, ISBN 87 7491 6912, ISSN 0909 - 4288, Road Directorate, Copenhagen, 1996.

Haugaard, M. & Berrig, A.: "HETEK - Curing - Supplementary Research, Proposal". Road Directorate, report No. 38, Copenhagen, 1996.

Riis, K. and Haugaard, M.: "HETEK - Curing - Phase 1: Laboratory Tests". Road Directorate, report No. 73, Copenhagen, 1997.

List of Symbols

W	Water content in concrete (kg/m^3)
C	Cement content in concrete (kg/m^3)
FA	Fly Ash content in concrete (kg/m^3)
MS	Micro Silica content in concrete (kg/m^3)
W/C$_e$	Effective water/cement ratio in concrete (kg/m^3) ($C_e = C + 0.5 \cdot FA + 2 \cdot MS$)
ß	Degree of hydration, by volume of cement
dU	Water loss by evaporation from concrete (kg/m^2)
dW	Water loss by evaporation from cement paste (m^3/m^3)
p_0	Porosity of cement paste at time of mixing (m^3/m^3)
$V_{cap=0}$	Volume ratio of (cement + gel) in cement paste, when capillary water content becomes zero

NB: In this project the maturity is defined as zero at the time of mixing.
The following abbreviations are used:
Mday = maturity days
Mh = maturity hours.

Appendices

Appendix A

Eq. W/C, air content and slump of the delivered concrete (recipe no. 6021).

Specimen no.	Equivalent water-cement ratio	Air content [%]	Slump [mm]
1	0.37	5.7	100
2	0.37	5.7	100
3	0.38	5.8	140
4	0.39	6.7	80
5	0.38	7.0	130
6	0.38	7.0	130
7	0.38	6.7	90
8	0.38	6.7	90
9	0.39	6.5	120
10	0.39	6.7	80
11	0.39	6.1	90
12	0.39	6.1	90
13	0.39	6.5	90
14	0.39	6.5	90

Appendix B

The climatic condition during the first 10 Mdays (evaporation test)

Specimen no.	Temperature °C	Relative Humidity %	Wind velocity m/s
1	22	63	3.6
2	22	63	3.6
3	20	67	-
4	20	67	3.6
5	20	66	3.6
6	20	66	3.6
7	20	44	3.6
8	20	44	3.6
9	20	67	3.6
10	20	67	3.5
11	20	68	3.7
12	20	68	3.7
13	20	67	3.6
14	20	67	3.6

Appendix C

Weight losses

Specimen no.	Plywood kg/m²	Free surface kg/m²	Curing compound kg/m²	10 mm Foam-matt kg/m²	Wet surface kg/m²
1	0.04	0.47	-	-	-
2	0.00	0.08	0.14	-	-
3	0.04	-	-	-	-
4	-	3.39	-	-	-
5	0.01	0.90	-	-	-
6	0.00	0.17	0.15	-	-
7	-	3.56	-	-	-
8	0.01	0.06	0.16	-	-
9	-	0.84	0.30	-	-
10	-	0.55	-	-	-1.22
11	0.03	0.23	-	0.01	-
12	0.01	0.06	-	0.01	-
13	-	0.60	-	0.06	-
14	-	0.14	0.20	-	-

Appendix D

Micro analysis

Specimen no.	C mm	C along crack mm	Micro-crack ⊥	Micro-crack =	Fine crack ⊥	Fine crack =
1	0.4	2.1	4.3	0.0	0.0	0.0
2	0.5	2.1	5.3	0.0	0.0	0.0
3	0.5	3.2	2.6	0.0	0.0	1.0
4	4.0	0.0	3.0	5.3	0.0	0.3
5	1.7	0.0	0.6	0.0	0.0	0.0
6	0.3	2.2	5.3	0.0	0.6	0.0
7	3.6	0.0	0.0	0.0	0.0	0.0
8	0.0	0.0	0.0	0.0	0.0	0.0
9	0.1	0.0	1.3	8.0	1.0	10.0
10	0.4	2.1	5.6	6.0	1.3	2.3
11	0.5	0.8	2.6	0.0	0.6	0.0
12	0.2	0.4	0.3	0.0	0.3	0.3
13	0.6	2.1	1.6	1.0	0.0	2.6
14	0.4	2.3	0.6	4.6	0.0	0.0

Appendix E

Chloride penetration

Chloride penetration		
Specimen no.	Chloride penetration [Coulombs]	Curing methods
8	951	Mould in 3 Mdays + Curing compound - 44% RF
10	983	Water cured
14	985	Curing compound after 2 Mh
1	1013	Mould in 3 Mdays
2	1049	Mould in 3 Mdays + Curing compound
12	1059	Mould in 3 Mdays + Foam-matt
11	1084	Mould in 1 Mday + Foam-matt
13	1463	Foam-matt after 5 Mh
6	1556	Mould in 1 Mday + Curing compound
9	1711	Curing compound after 5 Mh
5	1717	Mould in 1 Mday
3	2239	Mould in 10 Mdays
4	>4000	Free surface
7	>4000	Free surface - 44% RF

Appendix F

Capillary water absorption, TI-B 25

Specimen no.	Porosity [vol-%]	Degree of saturation start	Degree of saturation	Period of saturation [Hours]
1	15.7	0.04	0.61	5.6
2	15.1	0.03	0.63	8.1
3	14.5	0.15	0.53	4.0
4	18.7	0.07	0.48	5.3
5	16.0	0.14	0.41	3.5
6	16.9	0.15	0.42	3.2
7	15.9	0.13	0.40	7.3
8	14.7	0.31	0.44	17.6
9	18.8	0.29	0.41	6.6
10	16.7	0.28	0.54	2.3
11	14.5	0.29	0.61	3.6
12	14.1	0.34	0.56	3.4
13	16.3	0.21	0.50	4.0
14	15.8	0.28	0.43	15.2

Appendix G

Carbonation depth (mm)

Specimen no	1 month d_k	1 month d_{max}	2 month d_k	2 month d_{max}	3 month d_k	3 month d_{max}
1	0	0	3	4	3	5
2	0	0	3	3	3	5
3	6	9	9	10	10	12
4	16	19	20	23	25	26
5	7	8	9	11	11	13
6	4	5	6	8	8	9
7	14	17	21	25	22	25
8	0	0	0	0	0	3
9	4	6	4	6	8	10
10	3	5	5	11	5	7
11	5	7	7	11	8	10
12	3	6	4	6	5	9
13	3	5	3	4	3	4
14	0	0	0	2	0	0